Geological Quarterly, 2021, 65: 52
DOI: http://dx.doi.org/10.7306/gq.1621

Sedimentary environments and stratigraphy of the Stipinai Formation (Upper Frasnian, northern Lithuania): a sedimentary record of sea-level changes in the Main Devonian Field of the East European Platform

Piotr JAGLARZ[1, *], Tomasz RYCHLIŃSKI[1], Paweł FILIPIAK[2], Alfred UCHMAN[1] and Julius VAINORIUS[3]

[1] Jagiellonian University in Kraków, Faculty of Geography and Geology, Institute of Geological Sciences, Gronostajowa 3a, 30-387 Kraków, Poland

[2] University of Silesia in Katowice, Faculty of Natural Sciences, Institute of Earth Sciences, Będzińska 60, 41-200 Sosnowiec, Poland

[3] Šiauliai Aušros Museum, Vilniaus St. 74, LT-76283 Šiauliai, Lithuania

Jaglarz, P., Rychliński, T., Filipiak, P. Uchman, A., Vainorius, J., 2021. Sedimentary environments and stratigraphy of the Stipinai Formation (Upper Frasnian, northern Lithuania): a sedimentary record of sea-level changes in the Main Devonian Field of the East European Platform. Geological Quarterly, 65: 52, doi: 10.7306/gq.1621

The Frasnian carbonate-siliciclastic deposits of the Stipinai Formation exposed in two quarries at Petrašiūnai and Klovainiai (northern Lithuania) show considerable vertical facies changes. The lower part of this succession is dominated by argillaceous dolomitic facies with subordinate fine siliciclastic deposits. They display haloturbation and bioturbation structures, represent a hypersaline lagoonal environment, and record the beginning of the transgression. The middle part of the succession consists of secondary dolostones containing moulds of brachiopods, tetracorals, stromatoporoids and trace fossils of deposit feeders; these were deposited in a shallow subtidal marine environment and represent the deepest sedimentary environment of this succession. This was followed by a lagoonal environment (episodic hypersaline), represented by dolomudstones and marly dolomudstones. The upper part of the succession is built of bedded dolostones which document a shallowing trend. Intercalations of clays and palaeosol horizons record emergence events. Palynostratigraphic data tentatively indicate that the Stipinai Formation represents the Upper Frasnian. The succession can be interpreted as a record of the upper part of a T-R cycle (related to the *semichatovae* transgression) in the Main Devonian Field of the East European Platform. The Stipinai Formation is distributed across western and central Latvia and has a correlative in the Pomerania Basin (northern Poland).

Key words: facies, dolostones, relative sea-level changes, palynostratigraphy, Baltic Basin, Upper Devonian.

INTRODUCTION

The Devonian Baltic Basin (Pontén and Plink-Björklund, 2009) or Baltic Devonian Basin (Lukševičs et al., 2011) was formed as a consequence of the collision of eastern Avalonia and Baltica in the Late Ordovician (Poprawa et al., 1999). During the Devonian, its northwestern part was uplifted and eroded, while in its central and eastern part, two NE–SW trending depocentres developed in which intermittent continental, deltaic, estuarine, lagoonal and shallow marine sedimentation took place (e.g., Paškevičius, 1997; Ūsaitytė, 2000; Lukševičs et al., 2012; Stinkulis et al., 2020). This sedimentation was controlled by eustatic sea level changes at subequatorial latitudes (Bachtadse et al., 1995; Bełka and Narkiewicz, 2008). The exposures of the Frasnian Stipinai Formation in northern Lithuania studied here give an opportunity to investigate Upper Devonian facies variability in the Baltic Basin and the causes of palaeoenvironmental changes during Frasnian time. The main goal of the paper is the determination of age of the Stipinai Formation via palynostratigraphy, and interpretation of facies changes through the succession. The stratigraphical data allow correlation of the Stipinai Formation facies changes to the global sea-level curve (see Dopieralska et al., 2016).

GEOLOGICAL BACKGROUND

The Upper Devonian sections examined are located in northern Lithuania (Fig. 1A) in the western part of the Main Devonian Field of the East European Platform (Vodzinskas and Kadūnas, 1969). The Main Devonian Field constitutes the largest Devonian outcrops and subcrops in Europe, encompassing southern Estonia, Latvia, northern Lithuania, as well as the adjacent parts of Russia and the Baltic Sea. Structurally, this area belongs to the Baltic Syneclise (Paškevičius, 1997; Bełka and

* Corresponding author, e-mail: piotr.jaglarz@uj.edu.pl

Received: April 6, 2021; accepted: October 23, 2021; first published online: November 29, 2021

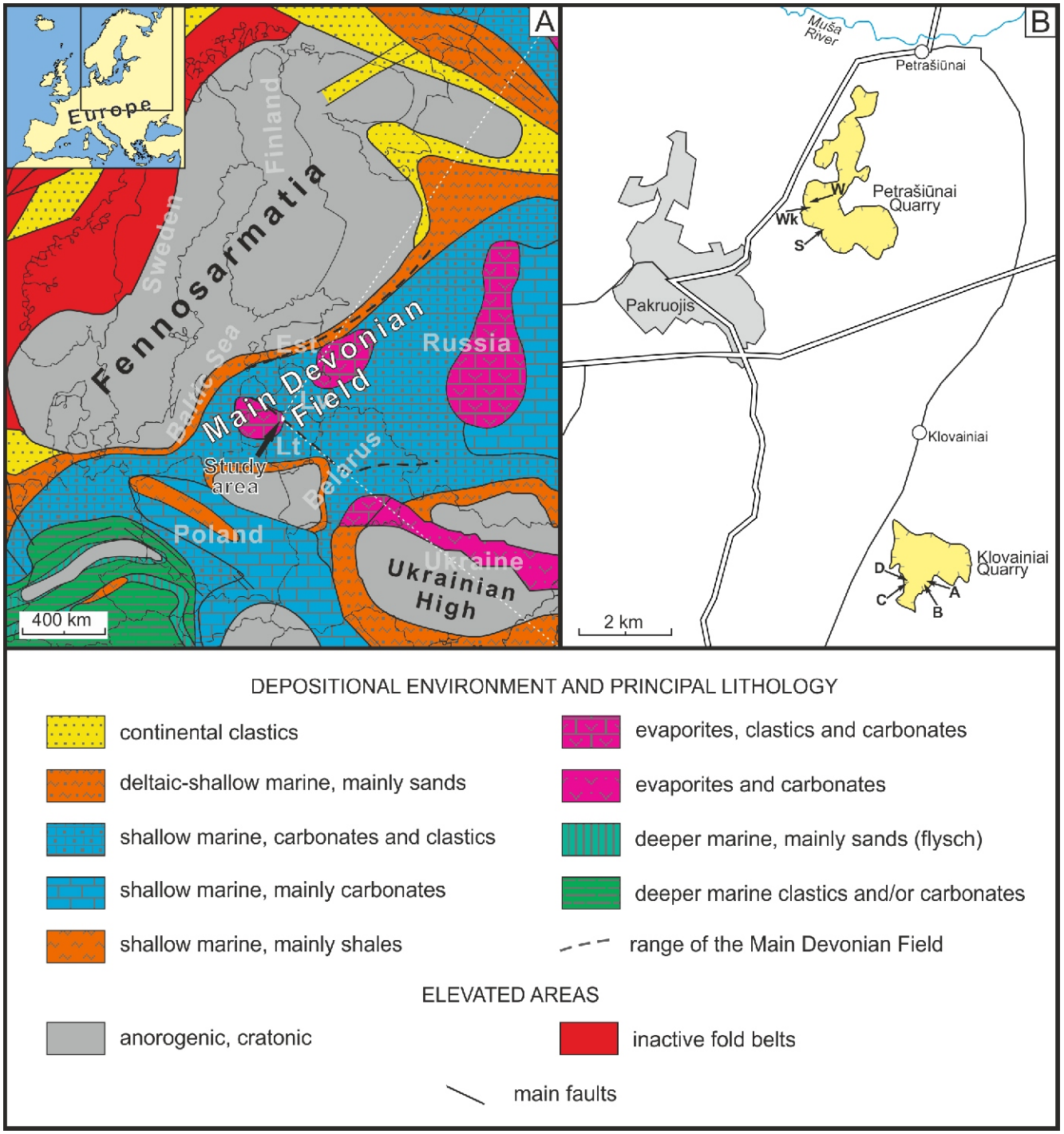

Fig. 1. Location of the study area

A – palaeogeographic-palaeotectonic sketch-map of northeastern Europe during the Late Devonian with location of the study area: Lt – Lithuania, Lv – Latvia, Est – Estonia (after Ziegler, 1988, modified); **B** – detailed map with the location of the quarries and sections studied

Narkiewicz, 2008). The study area is located in the southeastern part of the Baltic Syneclise, termed the Polish-Lithuanian depression, which was formed during the Late Permian (Paškevičius, 1997).

During the Devonian, the area of the recent Main Devonian Field was a part of the Baltic Basin, which developed in the western part of the East European Platform on the Laurussia continent. During the earliest Devonian, continental-lagoonal sedimentation prevailed in the Baltic Basin except for its northern part, which was uplifted and eroded (Paškevičius, 1997). Sandstone-dominated siliciclastic sediments were deposited from the Pragian until the end of the Givetian (Tänavsuu-Milkeviciene et al., 2009). During the Pragian and Emsian, these sediments accumulated on river deltas and in lakes (Paškevičius, 1997). From the latest Emsian to Givetian, deposition occurred in a tidally influenced delta or in a tide-dominated estuary (see Pontén and Plink-Björklund, 2009; Tänavsuu-Milkeviciene et al., 2009; Lukševičs et al., 2012). However, during the Eifelian, siliciclastic deposition was interrupted by an episode of mixed carbonate-siliciclastic marine accumulation (Tänavsuu-Milkeviciene et al., 2008, 2009).

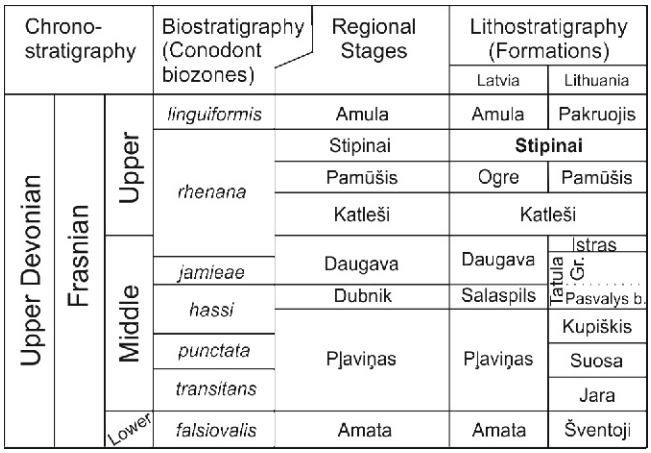

Fig. 2. Current stratigraphy of the Frasnian stage in Latvia and Lithuania (compiled from Paškevičius, 1997; Lukševičs et al., 2012; Stinkulis et al., 2020)

The Frasnian is divided into several regional stages (RS; Fig. 2). The lower Frasnian Amata RS is represented by the Amata Formation in Latvia and the uppermost part of the Šventoji Formation in Lithuania (Tänavsuu-Milkeviciene et al., 2009; Lukševičs et al., 2012; Stinkulis et al., 2020). The succession is composed of fine-grained sandstones, siltstones and claystones deposited in tide-dominated estuaries (Pontén and Plink-Björklund, 2009; Lukševičs et al., 2012). The Pļaviņas RS is represented by the Pļaviņas Formation in Latvia and by three formations in Lithuania (Paškevičius, 1997; see Fig. 2). The lower part of the succession consists of dolomitic marlstones, claystones, sandstones and dolostones, and the upper part of the Pļaviņas Formation is dominated by dolostones. Invertebrate fossil-rich limestones (commonly dolomitized) represent an open marine sedimentary environment. By contrast, dolomitic marlstones, dolostones and gypsum lenses were deposited in hypersaline lagoons in a more restricted part of the basin (Paškevičius, 1997; Lukševičs et al., 2012). The Salaspilis Formation in Latvia and the Pasvalys Beds (lower part of the Tatula Group) in Lithuania originated during the Dubnik RS. They are dominated by dolostones, dolomitic marlstones, claystones and gypsum (Paškevičius, 1997). These deposits were formed in a hypersaline lagoon or sabkha (Lukševičs et al., 2012). The Daugava RS is represented by the Daugava Formation (Latvia) and the upper part of the Tatula Group and the Istras Formation (Lithuania). The Daugava Formation consists of cavernous dolostones, organogenic limestones, dolomitized limestones, dolostones, clays, and gypsum. The Tatula Group is dominated by dolostones, dolomitic marlstones, claystones and gypsum, and the Įstras Formation is composed mostly of dolostones and gypsum (Paškevičius, 1997). The Daugava Formation is dominated by deposits representing a nearly normal salinity shallow-marine environment, while the Tatula Group containing gypsum beds represents a hypersaline lagoon environment (Paškevičius, 1997; Lukševičs et al., 2012). Deposits of the Įstras Formation represent a restricted shallow-marine environment (Paškevičius, 1997). The Katleši RS is represented by the Katleši Formation (Paškevičius, 1997; Fig. 2). The lower part of the formation comprises five cycles. Each of these is composed of sandstones or dolostones in the lower part, and carbonate claystones or dolomitic marlstones in the upper part. The uppermost part of the Katleši Formation consists of claystones, clayey siltstones, dolomitic marlstones, and local dolocretes (Lukševičs et al., 2012). The Pamūšis RS is represented by the Ogre Formation in Latvia and the Pamūšis Formation in Lithuania (Paškevičius, 1997). The Ogre Formation is composed of sandstones, siltstones and claystones (Lukševičs et al., 2011; Stinkulis et al., 2020). These deposits accumulated in deltaic or estuarine environments (Stinkulis et al., 2020). By contrast, the Pamūšis Formation is composed of marlstones with interlayers of gypsum, claystones, siltstones, sandstones, marlstones and dolostones (Lukševičs et al., 2012). These deposits were formed in hypersaline to normal saline lagoonal environments (Paškevičius, 1997). The Stipinai Formation was deposited during the Stipinai RS. Besides northern Lithuania, this formation is distributed across western and central Latvia (Lukševičs et al., 2012). The lower part of the succession is dominated by alternating dolostones, clayey dolostones and dolomitic marlstones (Paškevičius, 1997; Lukševičs et al., 2012), but sandstone and siltstone interlayers occur in the lowermost part of the Stipinai Formation (Lukševičs et al., 2012; Rychliński et al., 2014). Dolostones, often with skeletal fossils (brachiopods, bryozoans, stromatoporoids and rugose corals), dominate in the upper part of the Stipinai Formation (Paškevičius, 1997). In the uppermost part of the succession, the clay content increases (Lukševičs et al., 2012). The Amula RS is represented by the Amula Formation and by the Pakruojis Formation in Latvia and Lithuania, respectively (Paškevičius, 1997). The Pakruojis Formation is composed of dolomitic marlstones with gypsum, dolostones, marlstones, siltstones and sandstones. The Amula Formation consists of silty and sandy dolostones or alternating sandstones, siltstones and silty dolostones with variegated claystones, clayey siltstones, dolomitic marlstones and dolostones. Layers of gypsum-rich dolostone and gypsum also appear in this formation (Lukševičs et al., 2012). During Amula RS times, sedimentation took place in a hypersaline lagoonal environment (Paškevičius, 1997). The local Famennian Stage is composed of intercalating carbonaceous deposits (organodetrital limestones, marlstones and dolostones) and terrigenous siliciclastic deposits (sandstones and claystones; Ūsaitytė, 2000). The entire Upper Devonian succession of the Baltic Basin is up to 500 m thick (see Bełka et al., 2010).

The rocks examined are exposed in the Petrašiūnai and Klovainiai quarries (Pakruojis District, northern Lithuania) and belong to the Upper Devonian (Frasnian) Stipinai Formation (Bičkauskas and Radzevičius, 2014). The lowermost part of the section is composed of silty dolostones and calcareous silty arenites interlayered with dolomitic marlstones (Fig. 3). The calcareous silty arenites include well-preserved casts of halite crystals, indicating hypersaline conditions (Rychliński et al., 2014). The upper part of the section is dominated by dolostones, and marly dolostones with dolomitic mudstone intercalations. The dolostones (mainly dolowackestones and dolofloatstones) contain normal marine skeletal fossils, including tetracorals, brachiopods and gastropods (Sorokin, 1978; Paškevičius, 1997). The succession of the Stipinai Formation is topped by dolocretes interlayered with claystones. Marly dolomudstones occurring above the deposits of the Stipinai Formation probably belong to the Pakruojis Formation. The thickness of the Stipinai Formation in the study area does not exceed 21.5 m (Paškevičius, 1997; Narbutas, 2005). In the study area, the Devonian rocks are overlain by Quaternary sands and till, a few metres thick.

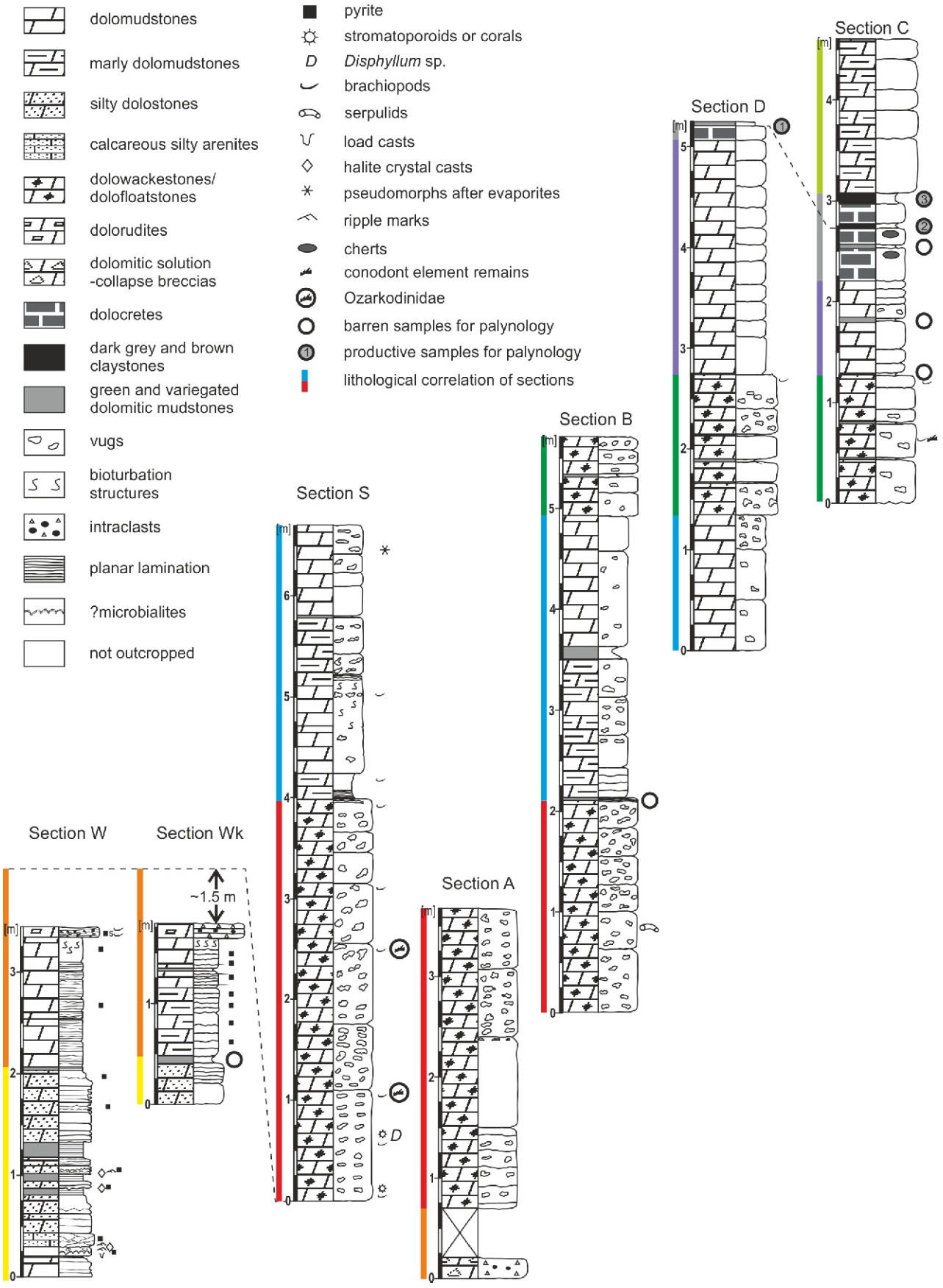

Fig. 3. Lithological logs of Frasnian deposits from the Petrašiūnai Quarry (W, Wk, S) and Klovainiai Quarry (A–D) and their correlation

MATERIALS AND METHODS

The succession was investigated bed-by-bed in seven individual sections. Three of these (sections W, Wk and S; their GPS coordinates are: E23°54.344', N55°59.586'; E23°54.331', N55°59.620'; E23°54.739', N55°59.379', respectively) are located in the Petrašiūnai Quarry while the next four (sections A, B, C, D; their GPS coordinates are: E23°56.674', N55°55.289'; E23°56.633', N55°55.267'; E23°56.274', N55°55.281'; E23°56.313', N55°55.307', respectively) are in the Klovainiai Quarry (Fig. 1B). Detailed lithological logs of these sections are shown in Figure 3. The thickness of the succession studied attains 18.5 m. Hand specimens, collected bed by bed, were subject to laboratory analysis. A hundred thin sections were made for detailed microfacies analyses. Selected uncovered thin sections were impregnated under vacuum with blue-stained epoxy resin, one for staining with alizarin red S and potassium ferricyanide solution (Dickson, 1966), and the other for double polishing and study under cathodoluminescence (CL). The CL petrography was performed using a *Technosyn Model 8200 Mark III* cold-cathode instrument (Technosyn Limited, Cambridge, UK), mounted on a binocular petrographic microscope (*Nikon Eclipse 50i*) equipped with 4x and 10x objectives and a trinocular photohead with 10x oculars. It allows real-time visual examination and analogue photomicrography, at magnifications of 40 to 100. Operating voltages were held at 14 to 16 kV and gun current levels at 450 to 550 μA. Dunham's (1962) classification as modified by Embry and Klovan (1971) was used for description of carbonate textures. Classification of dolomite texture is after Sibley and Gregg (1987) while classifications of breccia are based on the scheme proposed by Morrow (1982). The rock specimens illustrated are housed in the Nature Education Centre of the Jagiellonian University in Kraków (CEP) – Museum of Geology (collection INGUJ267P).

A few samples of dolostones with bioclasts were dissolved in buffered formic acid following the procedure described by Jeppsson and Anehus (1995) for conodont extraction. Three of these included conodont remains (Fig. 3). The residues and extracted conodont elements are housed in the Nature Education Centre of the Jagiellonian University in Kraków (CEP) – Museum of Geology (collection INGUJ267P).

Seven weakly compacted clay samples (sections: Wk, C and D; Fig. 3) and one carbonate sample (section B; Fig. 3) were processed for palynology. Three of these from the Klovainiai Quarry were positive (section D – 1 and section C – 2, 3; Fig. 3), while five had no organic residue. The standard laboratory procedure was applied, using the HCl-HF-HCl acid sequence (e.g., Wood et al., 1996). The kerogen obtained was sieved through 20 μm mesh nylon sieves. In addition, a part of the organics (samples 2 and 3) were treated with fuming nitric acid (100%) to remove amorphous organic matter (AOM). Petropoxy 154 was used as a mounting agent. Six slides per sample were prepared for palynological studies: four without amorphous substance for palynostratigraphy and two with complete organic content for palynofacies observation. Generally, the organic matter is very well preserved. Observation and documentation were completed using a transmitted light microscope (*Nikon Eclipse 50i* with a *DS-U3* controller and *Nikon NIS-Elements* imaging software suite). The residues and palynological slides are housed in the Institute of Earth Sciences (Sosnowiec), University of Silesia in Katowice, Poland.

RESULTS

FACIES DESCRIPTION

The carbonate rocks investigated (especially from the middle part of the succession studied) have been significantly altered by diagenetic processes (dolomitization and dedolomitization, dissolution, silicification; Fig. 4A, D–F). Dissolution vugs are diverse in shape and size, up to 5 cm across with irregular margins, chaotically arranged or locally parallel to the bedding surfaces. Some of the vugs resulted from dissolved bioclasts, while others may be transformed burrows. The basal parts of some vugs are filled with marly yellowish material. Despite the diagenetic transformations, a few distinct lithofacies can be distinguished. These are based mostly on macroscopic features and are supplemented by microscopic data from thin sections.

Dolowackestones/dolofloatstones. This facies are present in sections S, A, B, C and D (Fig. 3). It is represented by grey and yellowish-grey, medium to thick-beds of dolostone, which are up to 100 cm thick (Fig. 4A). This facies is composed of recrystallized micrite, brachiopod shells showing "ghost" preservation, corals and stromatoporoids, poorly preserved bioclasts (?foraminifers), peloids and micrite intraclasts. Conodont elements (Figs. 3 and 5) and small grains of detrital quartz (0.025–0.1 mm in diameter) are locally present. The dolomite crystals which have replaced micrite are cloudy, while the crystals which have replaced brachiopod shells are larger and mostly limpid (Fig. 6B). Vugs are common. Some of these are internal moulds of corals (in places with visible morphology of epitheca and septal furrows, see Fig. 4D), brachiopods and gastropods (Fig. 4B).

Dolomudstones and marly dolomudstones are present in all sections (Fig. 7A). This facies is built of greenish-grey and yellowish-grey planar-laminated micritic dolomudstones, which are bioturbated and nodular in places. In section S, they contain rare pseudomorphs after evaporites (Fig. 3). The content of detrital material (quartz grains, muscovite flakes and clay particles) is variable, up to 5% of the rock volume. The size of quartz grains and muscovite flakes varies from 0.03 to 0.10 mm across. The lamination results from the variable content of the detrital material.

Bioturbated dolomudstones dominate in the upper part of sections W and Wk (Fig. 7A, D). They are characterized by a lack of skeletal fossils. The degree of bioturbation is variable. Usually, totally and partially bioturbated layers alternate. In the latter, primary sedimentary structures, such as planar horizontal lamination, are partially preserved (Fig. 7D–E); the former are similar to those from the previously described facies. The dominant trace fossil is *Planolites* (Fig. 7C), which is filled with yellowish dolomudstone, and *Palaeophycus*. *Teichichnus*, ?*Chondrites* and ?*Rhizocorallium* are also present. The bioturbation structures are relatively shallow. They penetrate the sediment up to 3 cm from the colonization surface (see Fig. 7D). The nodular fabric resulted from pressure dissolution of the carbonates in the part of the rock enriched in clay minerals and from reprecipitation of carbonates in the carbonate-rich parts.

The pseudomorphs are small (up to 1.5 mm across), elongate, regular in shape and chaotically distributed (Fig. 6A). Although primary microfeatures are not well preserved, the de-

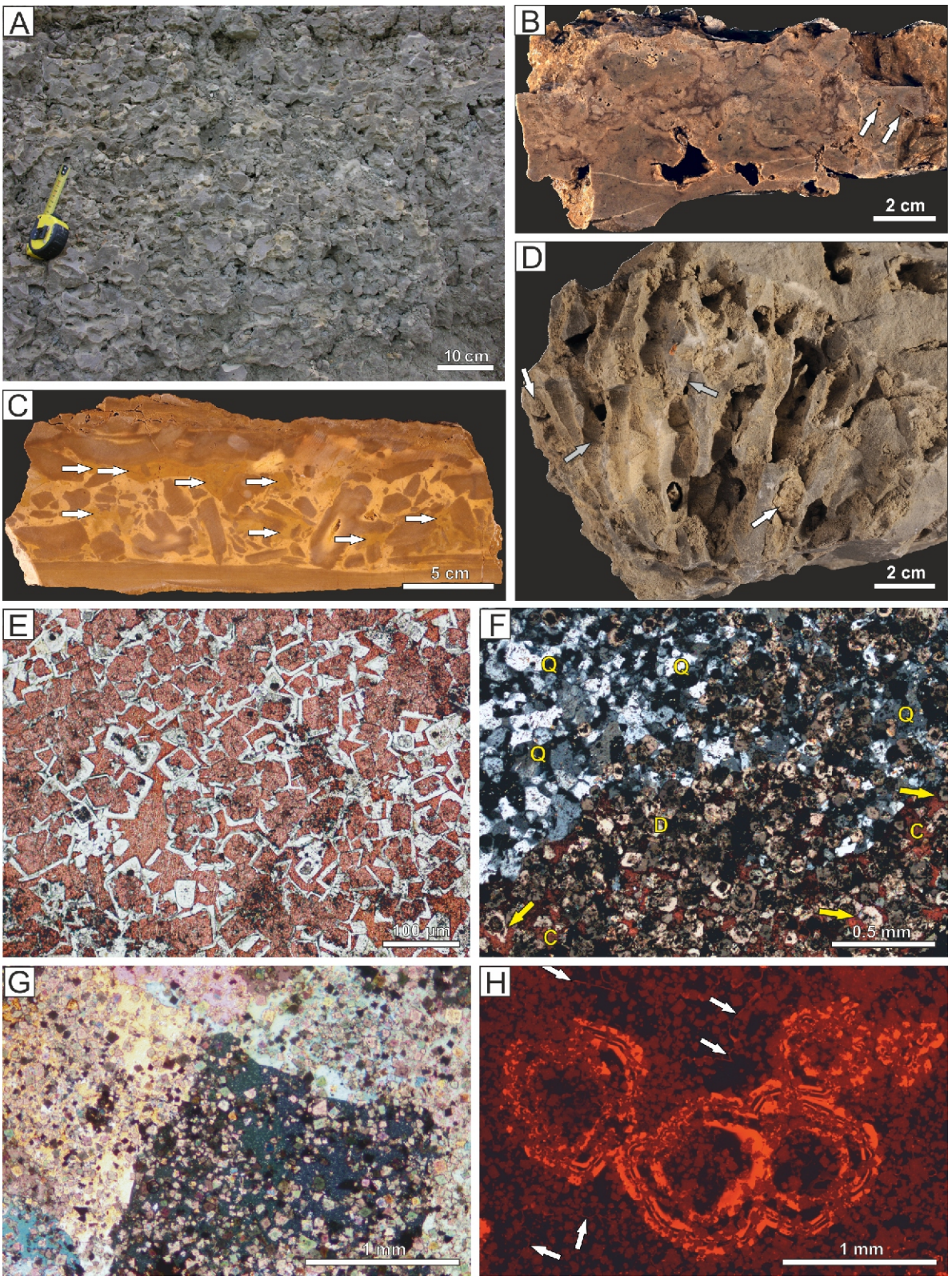

Fig. 4. Facies characteristics and diagenetic features of the Stipinai Formation

A – vuggy dolofloatstones/dolowackestones from the middle part of the section S, Petrašiūnai Quarry; **B** – strongly porous nodular dolostone with poorly preserved bioclasts (?gastropods; arrows), INGUJ267P9; **C** – solution-collapse breccia from the base of section A. Note the flat bottom of the breccia layer. Arrows indicate darker zones built of poikilotopic calcite cement, INGUJ267P6; **D** – vugs after the dissolved rugose coral *Disphyllum* sp. Coral remains preserved as casts (white arrows). The primary structure is partly preserved as internal moulds (white arrows) or casts (grey arrows), INGUJ267P8; **E** – planar-e mosaic dolomite with advanced dedolomitization progressing towards the crystal edges. Stained thin section (PPL), INGUJ267P11; **F** – silicified and dedolomitized dolostone. Inclusion-rich quartz crystals (Q), eu- to subhedral dolomite crystals with cloudy dedolomitized cores (D) and non-ferroan calcite (C) filling intercrystal space in the carbonates. Note corrosion of a dolomite crystal (arrows), INGUJ267P13; **G** – thin section of solution-collapse breccia matrix from Figure 4C. Note large crystals of poikilotopic calcite and scattered small euhedral dolomite crystals (XPL), INGUJ267P7; **H** – CL view of Figure 4G with visible relicts of large dolomite crystals (edges indicated by arrows) characterized by non-luminescent and bright-luminescent zones. Such dolomite is non-mimically replaced by euhedral dolomites and poikilotopic calcite

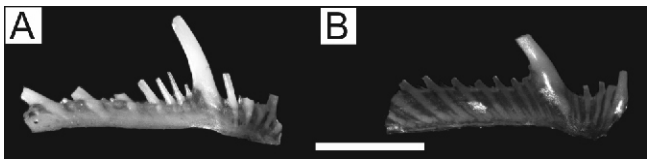

Fig. 5. Conodont elements

A, B – family Ozarkodinidae (cf. Sweet, 1988) – amber coloured ozarkodinid conodont Sc elements indicate Conodont Alteration Index (CAI) 1 (pers. comm. K. Narkiewicz, 2020); scale bar 500 μm; section S (see Fig. 3); INGUJ267P3 (A), INGUJ267P2 (B)

posits show some features of a primary dolomudstone, e.g. remnants of a micrite fabric preserved as "clouds" in a non-planar dolomite crystal mosaic. In turn, the dolomite crystals that fill pseudomorphs are twofold: they are limpid along the pseudomorph edges, while the crystals are cloudy in the centres of the pseudomorphs. The thickness of the dolomudstones with pseudomorphs after sulphates does not exceed 0.1 m.

Silty dolostones and calcareous silty arenites are restricted to sections W and Wk. They are light grey or yellowish and built of grains ranging from 0.03 mm to 0.13 mm across. The rock framework consists of quartz and feldspar grains and subordinate mica flakes. The beds show planar and wave-ripple cross lamination, which is disturbed in places by haloturbation structures such as sink-hole and dewatering pipes. Locally, halite crystal casts are visible on the lower (or rarely upper) bed surfaces. The lamination is emphasized by mica flakes and small pyrite crystals. Commonly, the rocks are cemented by poikilitopic calcite crystals (see Rychliński et al., 2014).

Intraformational breccias are present at the top of section W and Wk. They are characterized by a mud-supported fabric, monomictic texture, dark grey matrix and sharp, uneven erosive bases (Fig. 7D). The clasts are green-grey, and their maximum diameter does not exceed 2 cm. They are built of a nonplanar dolomite crystal mosaic, with crystals which are 50–100 μm across. The dark grey colour of the matrix results from the presence of pyrite crystals dispersed between the dolomite crystals. In section Wk, two levels of such breccias are present. The lower one is a float breccia which overlies bioturbated dolomudstones (Fig. 7D), and underlies a floatstone with intraclasts and moulds of dissolved bioclasts (mostly brachiopods) while the upper one is a pack breccia. Some intraclasts in the breccia are partially or completely pyritized. The intraformational breccia is up to 5 cm thick.

Solution-collapse breccias (present only in the basal part of section A) are intraformational, monomictic dolomitic breccias, up to 10 cm thick (Fig. 4C). They are characterized by sharp and almost even bases and indistinct, irregular, undulating tops. Clasts are beige-brown in colour and up to 5 cm across. They are chaotically arranged, poorly sorted and cemented with a yellowish dolomitic matrix and brown-yellowish calcite matrix. Their lithology is the same as that of the underlying and overlying rocks. Some clasts are cracked. The breccias are grain- to mud-supported and, in place, reveal weak graded bedding. The matrix is partly replaced by poikilitopic calcite spar cements (Fig. 4G, H). Crystals of non-ferroan calcite spar reach up to 3 mm across while smaller (up to 0.1 mm across) planar-e (euhedral) cloudy dolomite crystals form the "floating texture".

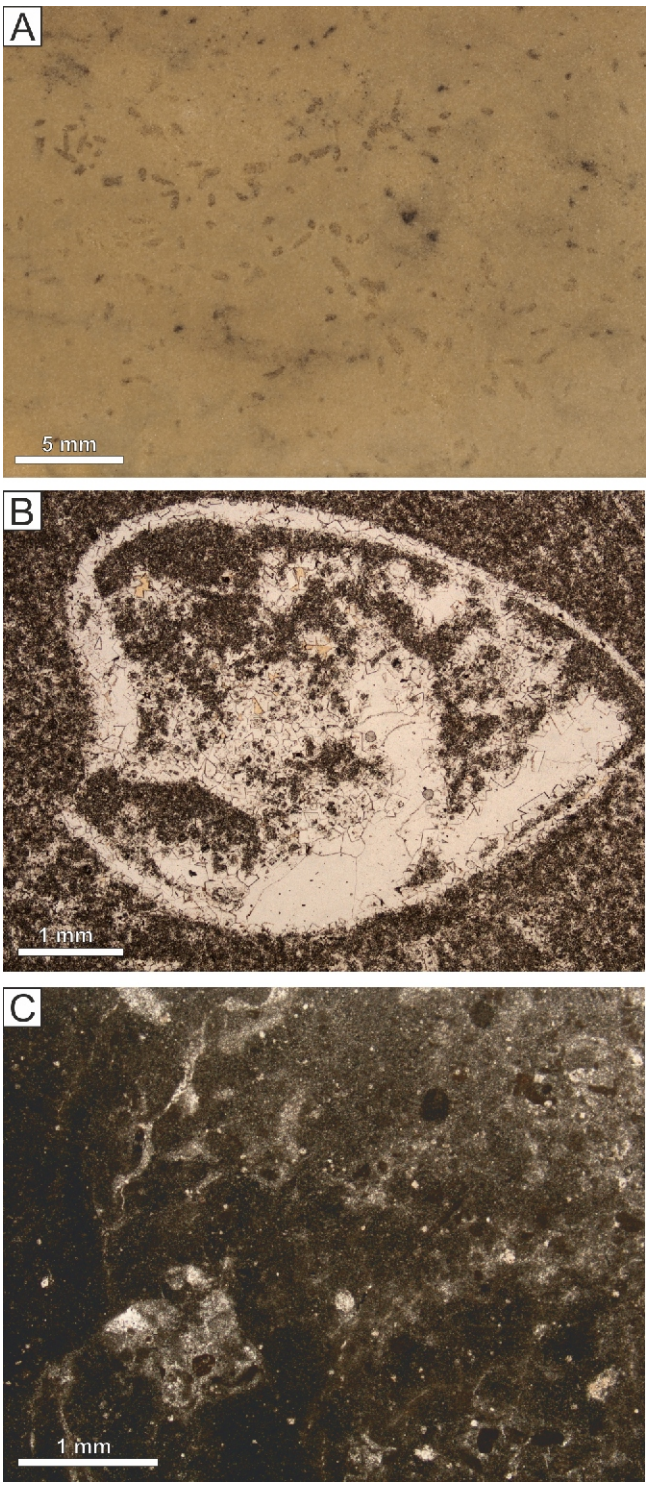

Fig. 6. Microfacies features of the Stipinai Formation

A – dolomudstone with scattered pseudomorphs after evaporites from the section S, INGUJ267P10; **B** – recrystallized bioclastic dolowackestone from the lowermost part of the section C with a brachiopod shell replaced by subhedral dolomite and blocky calcite spar, INGUJ267P12; **C** – dolocrete from section C (details of Fig. 7F), INGUJ267P15

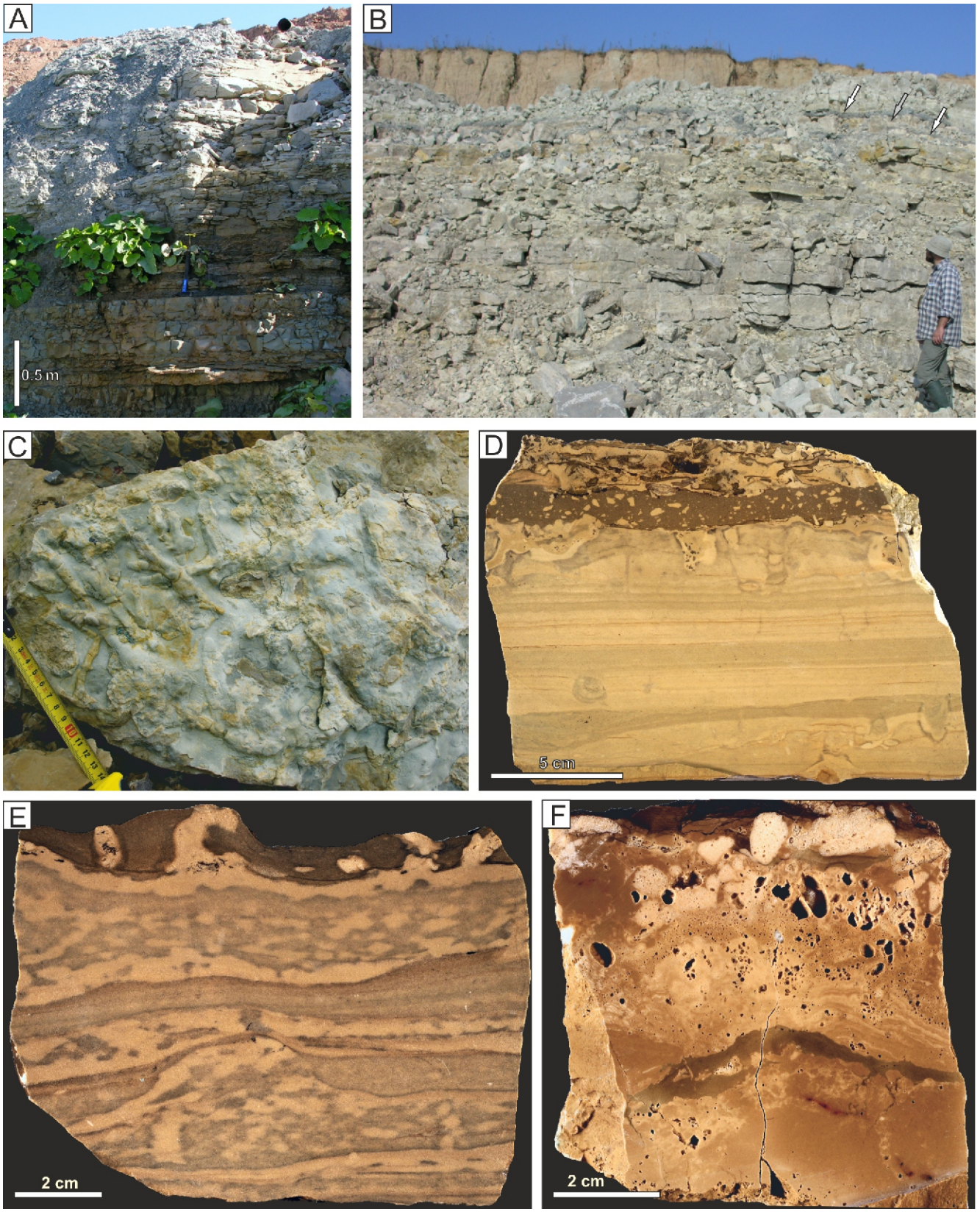

Fig. 7. Facies characteristics of the Stipinai Formation

A – lowermost part of the succession studied, built of silty dolostones with haloturbation structures and halite casts intercalated with dolomitic marlstones (section W); **B** – upper part of the Stipinai Formation – bedded dolostones intercalated with mudstones (white arrows), grey arrows indicate position of dolocrete shown in F, section C; **C** – trace fossil *Planolites*, uppermost part of section W; **D** – partly laminated dolomudstones with bioturbation structures, erosive mud-supported breccia and floatstone bed – uppermost part of the Wk section, INGUJ267P4; **E** – strongly bioturbated dolomudstones from the upper part of section W, INGUJ267P5; **F** – dolocrete from the uppermost part of section C, INGUJ267P14

Mudstones and claystones are restricted to the lower and upper parts of the succession discussed. Their thickness varies from 2.5 to 15 cm. The mudstones and claystones are mostly green or green-grey, rarely variegated or dark grey and brown (in section C) in colour. They are devoid of sedimentary structures, except for variegated mudstones which locally show planar lamination. In sections C and D, this facies overlies dolocretes.

Dolocrete facies are present in the upper part of the sections C and D (Fig. 7B, F). These facies are characterized by microfabrics related to subaerial exposure. In thin sections, typical features include crystallaria and rhombic calcite crystals, a dense microfabric and micrite nodules (Fig. 6C), that characterize the alpha-calcretes, and a biogenic fabric (alveolar septal structures) which is typical of the beta-calcretes (Wright, 1990). Rocks of this facies are overlain by claystones of the previously described microfacies. The thickness of dolocrete beds does not exceed 30 cm.

PALYNOFACIES

Three samples from the upper part of the section investigated from the Klovainiai Quarry yielded microfloral assemblages. Samples 2 and 3 contain a diverse miospore assemblage but sample 1 shows less diverse taxa and poorly preserved miospores (Fig. 3). Because sample 1 is partly weathered, there is little data from this material. Only single miospores in the residue were observed; a marked concentration of black crystals predominates (pyrite?), and AOM is absent.

The miospores obtained from samples 2 and 3 are very similar in taxonomic composition. Among these, *Auroraspora speciosa, Diducites radiatus* and *Membrabaculisporis radiatus* are frequent. Moreover, *Diducites mucronatus* and *Kedosporites imperfectus* (Fig. 8) are also present. The miospore assemblage is characterised by the dominance of *Geminonspora* spp., e.g. *G. aurita, G. notata*, *G. tuberculata* and *G. vasjamica*. Other miospore species include *Aneurospora greggsii*, *Ancyrospora voronensis, Contagisporites optivus*, *Cristatisporites deliquescens, Diaphanospora rugosa, Dictyotriletes* sp., *Diducites poljessicus, Hystricosporites* spp., *Kedosporites evlanensis*, *Stenozonotriletes cornformis* and *Verrucosisporites grumosus*. Importantly, a specimen similar to *Grandispora subsuta* (see Fig. 8) was also recorded.

A much poorer taxonomic assemblage was obtained from sample 1 (Fig. 3), which contains the miospores *Kedosporites* sp., *Archaeozontriletes* sp., *Retusotriletes* sp., and *Geminospora* sp.

Organic matter preserved only in samples 2 and 3 was analyzed in terms of palynofacies. In both samples structural organic components and abundant AOM were noted. Generally miospores predominated over other palynomorphs (Fig. 8). Phytoplankton is represented by prasinophytes, including *Leiospheridia*, *Hemiruptia* and *Pterospermella* (Fig. 9). A few algae coenobia *Musivum gradzinski* (Chlorococcales) were also recorded. No acritarchs and scolecodonts were found in the material analyzed. In sample 2, very few remains of terrestrial plant tracheids are visible (see Fig. 9), but in sample 3, higher plant tracheids are more abundant but still at a low level; most of these are preserved as charcoal particles (Fig. 9).

INTERPRETATION

SEDIMENTARY ENVIRONMENT

In general, most of the facies described represent a shallow marine, carbonate platform environment. The lowermost part of the succession described, including silty dolostones with haloturbation structures and halite crystal casts, laminated dolomudstones and bioturbated dolomudstones (lacking skeletal fossils) in the upper part of sections W and Wk represents hypersaline lagoonal deposits. Wave-ripple cross-laminated coarser-grained deposits with quartz grains and mica flakes which intercalate with dolomudstones were deposited probably during storms (Rychliński et al., 2014). The high amount of terrigenous material points to the proximity of the source area at that time. Salinity fluctuations in the sedimentary environment are reflected by the occurrence of beds with haloturbation structures, bioturbation structures and solution-collapse breccias in the lower part of the succession. Trace fossils from the bioturbated beds belong to the impoverished *Cruziana* ichnofacies (Pemberton et al., 2001; MacEachern et al., 2012). Low-diversity trace fossil assemblages and the low intensity of bioturbation, or high-density and the predominance of a single ichnotaxon, are typical features of marine restricted settings, with salinities higher than normal marine (de Gibert and Ekdale, 1999, 2002; Mercedes-Martin and Buatois, 2021). The formation of burrows was possible when the salinity decreased from strong hypersaline to moderate hypersaline conditions (cf. Jaglarz and Uchman, 2010).

An abrupt change in sedimentary regime is indicated by deposition of intraformational breccias alternating with floatstones including brachiopods (the upper part of sections W and Wk; Fig. 3). The fair-weather sedimentation of dolomudstones in a hypersaline environment was interrupted by event deposition referred to storms, which delivered water of normal salinity into the basin. This might be supported by the presence of solution-collapse breccias in the lower part of section A and by the first appearance of a marine skeletal fauna (section W; Fig. 3). The influx of normal marine waters caused dissolution of evaporites in the hypersaline lagoon environment. This might have led to formation of the breccias (section A; Fig. 4C) which show typical features of solution-collapse processes. These include lithology of the clasts being identical to the under- and overlying rocks, the sharp and even bases and indistinct and irregular tops of beds, and the chaotic arrangement and poor sorting of clasts (cf. Middleton, 1961; Eliassen and Talbot, 2005). The matrix might have originated by gravitational infiltration of overlying, unconsolidated, fine-grained sediments (Swennen et al., 1990; Jaglarz and Rychliński, 2018). The occurrence of mud-supported breccias indicates that the infiltration of fines and brecciation processes were simultaneous. This shows that the percolation of the waters into the underlying sediment and subsequent dissolution of the evaporitic beds caused collapse of the overlying early-cemented carbonate sediments at a relatively early stage of diagenesis. Above the breccia horizons, the deposits are dominated by dolostones containing normal marine fossils (e.g. brachiopods; section S), which points to normal marine salinity.

During deposition of the carbonates, the input of detrital material was significantly reduced. This corresponds to a marine transgression and indicates an increase in the distance from the provenance area (comp. Lukševičs et al., 2012). Because of the later diagenetic processes (mostly dolomitization), fossils in the dolomitic facies are poorly preserved, but corals, e.g. the tetracoral *Disphyllum* sp. (Paškevičius, 1997), stromatoporoids, gastropods, serpulids and brachiopods among others, e.g. *Theodossia semgalensis* Delle (Bičkauskas and Radzevičius, 2014), which are quite frequent in the lower part of the dolomitic facies, can be recognized. The carbonate deposits are bioturbated in places. The presence of stenohaline organism remains (e.g. corals) indicates a continuation of normal salinity conditions. In general, such conditions persisted throughout the deposition of the dolostones of sections S, A, B, D and the lower part of the section C though with one exception, when a few centimetres of dolomudstone with evaporite were

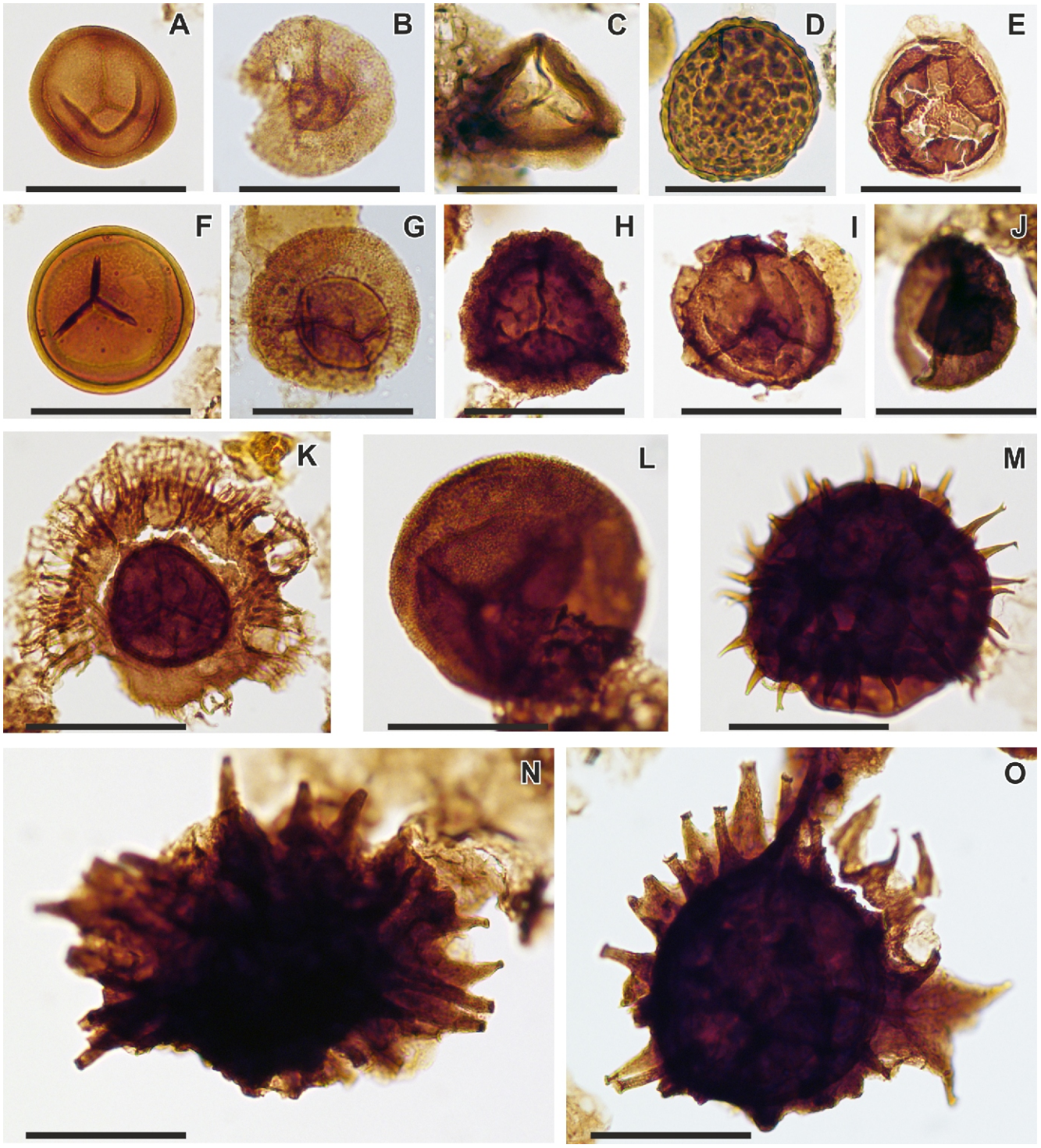

Fig. 8. Palynostratigraphically important and common miospores from the Klovainiai Quarry (section C)

A – *Geminospora aurita*; **B** – *Auroraspora speciosa*; **C** – *Kedosporis imperfectus*; **D** – *Verrucosisporites grumosus*; **E** – *Diaphanospora* sp.; **F** – *Stenozonotriletes conformis*; **G** – *Diducites radiatus*; **H** – *Cristatisporites deliquescens*; **I** – *Grandispora* cf. *subsuta*; **J** – *Diducites mucronatus*; **K** – *Membrabaculisporis radiatus*; **L** – *Contagisporites optivus*; **M** – *Hystricosporites* sp.; **N** – *Ancyrospora voronensis*; **O** – *Ancyrospora voronensis*; scale bar – 50 µm; **A**, **C–F**, **H–O**: sample 2; **B**, **G**: sample 3

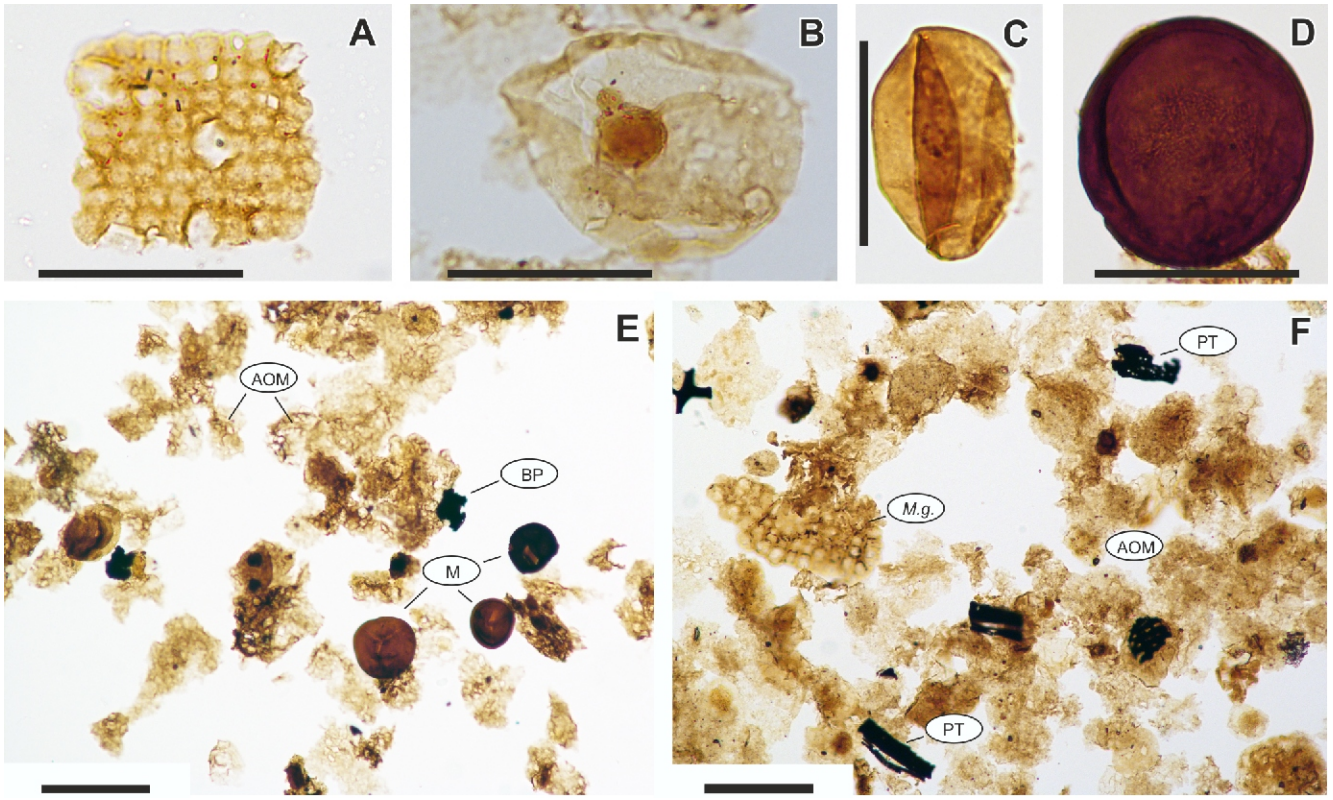

Fig. 9. Phytoplankton and palynofacies from the Klovainiai Quarry (section C)

A – *Musivum gradzinskii*; **B** – *Pterospermella* sp.; **C** – *Leiospheridia* sp.; **D** – *Hemiruptia* sp.; **E** – pictures of palynofacies, AOM predominate, some miospores (M) and small black organic particles (BP); **F** – pictures of palynofacies, AOM predominate, *Musivum gradzinskii* (*M.g.*) and higher plant tracheids (PT); **A–D**: scale bar – 50 μm; **E–F**: scale bar – 100 μm; **A–B**, **F**: sample 3; **C–E**: sample 2

formed (Fig. 6A). At that time, a short-term resumption of hypersaline conditions is postulated.

After deposition of the fossiliferous carbonates, the shallow-water carbonates were periodically emergent. This is shown by the presence of dolocretes with overlying layers of green and grey claystone, which are preserved at the top of section D and in the upper part of section C. The claystones are characterized by the presence of a strong concentration of AOM, well-preserved miospores, a small amount of higher plant tracheids and the absence of typical marine components such as acritarchs and scolecodonts. Cenobia of chlorophycean algae (Chlorococcales) are present; these are generally regarded as a fresh-water indicator (Wood and Turnau, 2001), although previous records of these algae also came from marine deposits of Givetian (Wood and Turnau, 2001) and Emsian age (Filipiak, 2011, 2014). Prasinophytes are regarded as an ambiguous fresh-water signal (Strother, 1996). Although Raskatova and Jurina (2012) estimated the amount of acritarchs to be 30% in coeval deposits (MR Subzone, Stipinai Fm.) of western Latvia, they use the term acritarch in a broad sense, also including prasinophytes (e.g. *Leiosphaeridia*). A typical acritarch mentioned by them (but without satisfactory quantitative data) is *Baltisphaeridium.* Thus, the upper part of the succession records shallowing of the sedimentary environment, which is further indicated by an increase in detrital content. The development of pedogenic processes related to episodes of sediment emergence records a marine regression resulting from sea-level fall.

Above the youngest pedogenic horizon in section C, the deposits are developed as marly dolostones. These include a much greater detrital content than do the underlying deposits and probably record the beginning of another marine transgression, which is referred to the Pakruojis Formation of the Amula Regional Stage (Fig. 2). However, this question cannot be unequivocally resolved because of erosional truncation and the lack of the younger Devonian deposits in the research area.

DISCUSSION

PALYNOSTRATIGRAPHY

The miospores obtained from samples 2 and 3 are very similar in taxonomic composition. According to Avkhimovitch et al. (1993), *Auroraspora speciosa, Diducites radiatus* and *Membrabaculisporis radiatus* appear for the first time in Eastern Europe in the CVe (*Cymbosporites vetlasjanicus*) Subzone (middle part of the OG (*Archaeoperisaccus ovalis – Verrucosisporites grumosus*) Miospore Zone, defined for the Middle Frasnian; Fig. 10) but their constant, more frequent presence is noticed from the succeeding MR (*Membrabaculisporis radiatus*) Subzone, until the end of the Frasnian. Moreover, *Diducites mucronatus* and *Kedosporites imperfectus* (Fig. 8) appear for the first time in the MR Subzone (Avkhimovitch et al., 1993). The presence of a specimen similar to *Grandispora subsuta* (see Fig. 8) could indicate the occurrence of the latest Frasnian DE (*Cristatisporites deliquescens – Verrucosisporites evlanensis*) Miospore Zone (GS – *Grandispora subsuta* Subzone; Fig. 10) but the single occurrence of this important taxon is uncertain here because the specimen is poorly preserved and other species indicative of this stratigraphic level were not recorded. There is an absence of the very distinctive

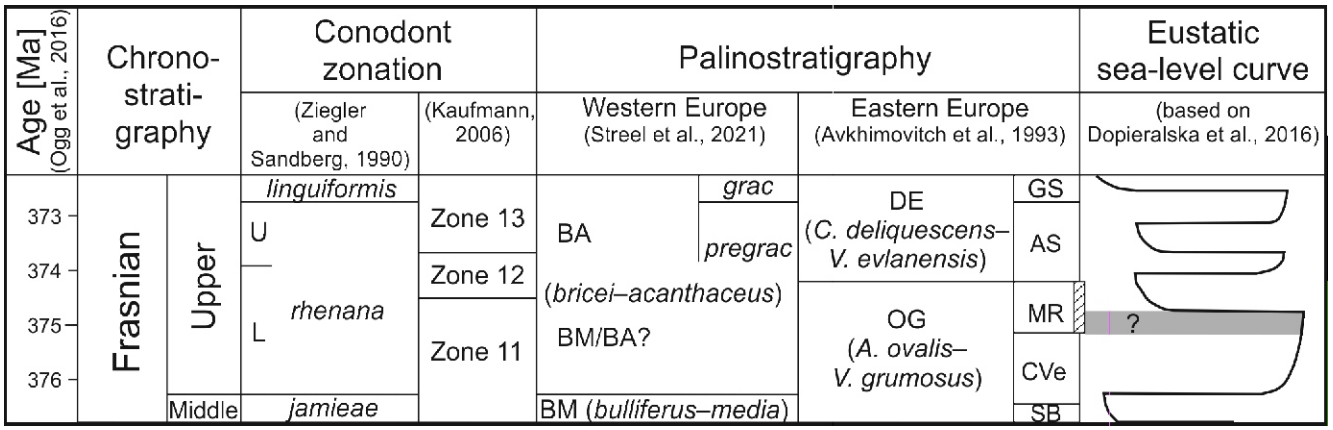

Fig. 10. Approximate correlation of the Upper Frasnian eustatic curve with conodont and miospore zones

Shaded field – stratigraphic range of the Stipinai Formation; striped field – the age of samples analyzed from the Klovainiai Quarry; BM, BA, OG, DE – miospore zones; SB, CVe, MR, AS, GS – miospore subzones

Archaeoperisaccus. According to Streel et al. (1987) and Richardson and McGregor (1986), this genus is typical of, and generally constantly present in, the Middle and in part the Upper Frasnian. However, Avkhimovitch at al. (1993) indicate that higher in the MR Subzone *Archaeoperisaccus* becomes less numerous. Raskatova and Jurina (2012) also mentioned the lack of *Archaeoperisaccus* in the Stipinai Formation of western Latvia.

Summarizing, the taxonomic composition of the miospore assemblage from samples 2 and 3 points rather to the MR Subzone (the youngest level of the OG Miospore Zone; Fig. 10; Avkhimovitch et al., 1993). Based on the current Frasnian miospore zonation updating by Streel et al. (2021), the Eastern Europe MR Subzone should be correlated with the unseparated BM (*Verrucosisporites bulliferus–Lophozonotriletes media*) / BA? (*Rugospora bricei–Cymbosporites acantheus*) microfloral level of western Europe (Fig. 10); and this, in turn, can be tentatively correlated with the *rhenana* Conodont Zone (Ziegler and Sandberg, 1990; for details see discussion in Streel et al., 2021: 77).

This dating is in agreement with the results of Raskatova and Jurina (2012) from the same lithostratigraphical unit (Stipinai Fm.) in western Latvia. A similar miospore assemblage occurs in both areas with no characteristic *Archeoperisaccus*. The presence of *Grandispora* cf. *subsuta* in the Klovainiai Quarry (sample 2; Fig. 8) may tentatively indicate the younger GS Subzone, from the latest Frasnian. However, this determination is weakened by the lack of taxa appearing from the AS (*Auroraspora speciosa*) Subzone and also by the lack of other taxa important for the GS Subzone (for detail see Avkhimovitch et al., 1993). In general, the small number of positive samples from the interval studied hampers unequivocal resolution of the age.

TRANSGRESSIVE-REGRESSIVE TRENDS

Well-preserved conodonts seem to be scarce, probably because of adverse environmental conditions. This precludes precise determination of the biostratigraphical age of the Stipinai Formation on the basis of the conodont zonation, though palynostratigraphy makes this possible.

Paškevičius (1997) included the stratigraphic range of the lithostratigraphic unit studied in the upper *Palmatolepis gigas* Zone. According to the current conodont zonation, the *P. gigas* Zone corresponds to the *P. rhenana* and *P. linguiformis* zones (Ziegler and Sandberg, 1990; Avkhimovitch et al., 1993; Streel et al., 2021). The taxonomic composition of the miospore assemblage indicates the MR Subzone (Fig. 10; Avkhimovitch et al., 1993). This subzone can be tentatively correlated with the *rhenana* levels in the conodont "standard" zonation (see Ziegler and Sandberg, 1990; Avkhimovitch et al., 1993; Streel et al., 2021) and therefore it indicates a Late Frasnian age for the Stipinai Fm. This dating is in general agreement with the results of Raskatova and Jurina (2012) from the same lithostratigraphic unit in western Latvia. Presumably, the Stipinai Formation corresponds to the Lower *rhenana* Zone, the stratigraphic range of which coincides with the duration of the upper part of the T-R cycle (Fig. 10).

The lower part of the succession represents a transgressive phase (Fig. 11). The dolomudstones and siltstones with haloturbation structures, planar lamination and trace fossils in the upper part of sections W and Wk (Fig. 7A, C–E) were deposited in a hypersaline lagoonal environment. The intraformational breccias preserved in the uppermost part of sections W and Wk define the first appearance of a skeletal marine fauna, although there is a small exposure gap just above this level. The overlying dolofloatstones and dolowackestones represent a normal marine and relatively deeper environment. The overlying marly dolomudstones and dolomudstones topped by green mudstones containing terrigenous material (sections S and B) represent a lagoonal environment related to marine regression. After that episode, as a result of deepening, carbonate sedimentation returned. This is manifested in the appearance of dolomudstones (including with pseudomorphs after evaporites; Fig. 6A), passing towards the sequence top into dolowackestones. The following regressive phase represents dolomudstones with mudstone intercalations, finally overlain by dolocrete horizons (Figs. 6C and 7A, B, F) which are intercalated with dark grey and green claystones (Figs. 3 and 7B) containing index miospores. The dolocrete and claystone package records sediment emergence. The overlying lagoonal marly dolostones record a transgressive phase of sea-level change and probably belong to the Pakruojis Formation of the Amula Regional Stage (Paškevičius, 1997).

The Stipinai Formation corresponds to the Lower *rhenana* Zone (Fig. 10). As index miospores were found at the top of the Stipinai Formation, it might be concluded that the formation probably represents the upper part of a T-R cycle corresponding to the so-called *semichatovae* transgression (Fig. 10; cf. Dopieralska et al., 2016).

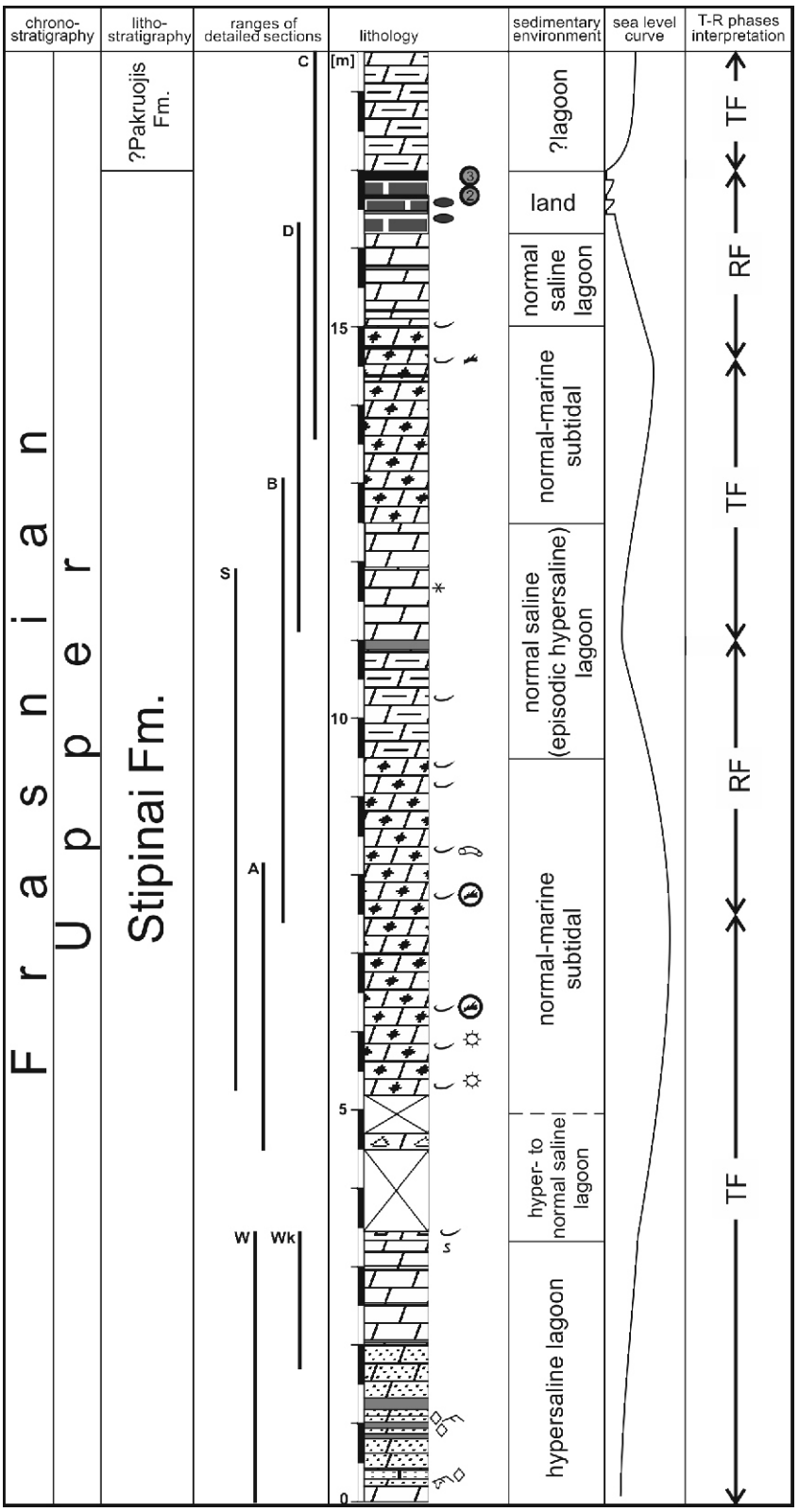

Fig. 11. Generalized lithological section of the Stipinai Formation with interpretation of sea-level fluctuations and phases of sea-level change

TF – transgressive phase, RF – regressive phase; other explanations as on Figure 3

During deposition of the Stipinai Formation, sedimentation took place in a relatively narrow basin (Paškevičius, 1997), which was presumably connected to the adjacent, normal marine Pomerania Basin (Matyja, 2006). In the western Pomerania region, platform and peri-platform carbonate deposits of the Koczała Formation correspond to the Stipinai Formation. In the same area, the beginning of the following T-R cycle is determined by a drowning episode of the carbonate platform and deposition of black offshore shales and deeper-water open shelf deposits (Matyja, 1993, 2006).

A record of the Frasnian marine transgressions is also observed in the areas adjacent to the Main Devonian Field. In the Central Devonian Field, they are represented by subtidal deposits with marine fossils, which are underlain and overlain by floodplain and marginal marine lagoonal deposits, respectively (cf. Alekseev et al., 1996; Zatoń et al., 2015).

CONCLUSIONS

Palynostratigraphic data indicate that the Stipinai Formation represents the Upper Frasnian (Lower *rhenana* Zone) and records the upper part of the T-R cycles related to the *semichatovae* transgression. Its rocks are extensively altered by diagenetic processes especially dolomitization, dedolomitization, dissolution and silicification. The lower part of the formation was deposited in a hypersaline lagoon environment, the middle part in a shallow water normal marine environment (open-marine subtidal to lagoonal) except for a short episode of higher salinity, while the upper part documents episodes of emergence and palaeosol development caused by a sea-level drop.

Vertical changes in the facies reflect two small-scale transgression events. The lower, carbonate-siliciclastic part of the succession as well as dolowackestones and dolofloatstones with marine organisms represents a transgressive phase of sea-level change. An episode of relative sea-level fall is recorded by marly dolomudstones and dolomudstones overlain by green mudstones. The overlying marly dolomudstones and mudstones with sporadic pseudomorphs after evaporites passing upwards to dolowackestones record relative sea-level rise. The following regressive phase is represented by dolomudstones with mudstone intercalations, finally overlain by horizons of dolocretes alternating with dark grey or green claystones.

Acknowledgements. We would like to thank O. Bábek (Palacký University Olomouc, Czech Republic), Z. Bełka (Adam Mickiewicz University, Poznań, Poland), A. Spiridonov (Vilnius University, Lithuania) and Ģ. Stinkulis (University of Latvia, Riga, Latvia) for critical and helpful reviewer comments. The authors are grateful to M. Melešytė (Vilnius University, Lithuania) for logistical support and to the management of Company Dolomitas, AB, Petrašiūnai and SC Klovainiai skalda for granting permission for the investigations. The research was supported by the Jagiellonian University in Kraków (DS fund). The authors are grateful to K. Narkiewicz (Polish Geological Institute – National Research Institute, Warszawa, Poland) for helpful remarks on the conodont element remains.

REFERENCES

Alekseev, A.S., Kononova, L.I., Nikishin, A.M., 1996. The Devonian and Carboniferous of the Moscow Syneclise (Russian Platform): stratigraphy and sea-level changes. Tectonophysics, **268**: 149–168.

Avkhimovitch, V.I., Tchibrikova, E.V., Obukhovskaya, T.G., Nazarenko, A.M., Umnova, V.T., Raskatova, L.G., Mantsurova, V.N., Loboziak, S., Streel, M., 1993. Middle and Upper Devonian miospore zonation of Eastern Europe. Bulletin des Centres de Recherches Exploration–Production Elf Aquitaine, **17**: 79–147.

Bachtadse, V., Torsvik, T.H., Tait, J.A., Soffle, H.C., 1995. Paleomagnetic constraints on the paleogeographic evolution of Europe during the Paleozoic. In: Pre-Permian Geology of Central and Eastern Europe (eds. R.D. Dallmeyer, W. Franke and K. Weber): 567–578. Springer, Berlin.

Bełka, Z., Narkiewicz, M., 2008. Devonian. In: The Geology of Central Europe, **1**: Precambrian and Palaeozoic (ed. T. McCann): 383–410. Geological Society, London.

Bełka, Z., Devleeschouwer, X., Narkiewicz, M., Piecha, M., Reijers, T.J.A., Ribbert, K.-H., Smith, N.J.P., 2010. Devonian. In: Petroleum Geological Atlas of the Southern Permian Basin Area (eds. J.C. Doornenbal and A.G. Stevenson): 71–79. EAGE Publications b.v, Houten.

Bičkauskas, G., Radzevičius, S., 2014. The Stipinai regional stage (Upper Devonian) in Petrašiūnai quarry. Geologija (Vilnius), **56**: 53–56.

de Gibert, J.M., Ekdale, A.A., 1999. Trace fossil assemblages refecting stressed environments in the Middle Jurassic Carmel Seaway of central Utah. Journal of Paleontology, **73**: 711–720.

de Gibert, J.M., Ekdale, A.A., 2002. Ichnology of a restricted epicontinental sea, Arpien Shale, Middle Jurassic, Utah, USA. Palaeogeography, Palaeoclimatology, Palaeoecology, **183**: 275–286.

Dickson, J.A.D., 1966. Carbonate identification and genesis as revealed by staining. Journal of Sedimentary Petrology, **36**: 491–505.

Dopieralska, J., Bełka, Z., Walczak, A., 2016. Nd isotope composition of conodonts: An accurate proxy of sea-level fluctuations. Gondwana Research, **34**: 284–295.

Dunham, R.J., 1962. Classification of carbonate rocks according to depositional texture. AAPG Memoir, **1**: 108–121.

Eliassen, A., Talbot, M. R., 2005. Solution-collapse breccias of the Minkinfjellet and Wordiekammen Formations, Central Spitsbergen, Svalbard: a large gypsum palaeokarst system. Sedimentology, **52**: 775–794.

Embry, A.F., Klovan, J.E., 1971. A Late Devonian reef tract on Northeastern Banks Island, NWT. Canadian Petroleum Geology Bulletin, **19**: 730–781.

Filipiak, P., 2011. Palynology of the Lower and Middle Devonian deposits in southern and central Poland. Review of Palaeobotany and Palynology, **166**: 213–252.

Filipiak, P., 2014. Palynology of the Lower and Middle Devonian clastic rocks from the Trojanowice 2 borehole (southern Poland) (in Polish with English summary). Biuletyn Państwowego Instytutu Geologicznego, **459**: 7–32.

Jaglarz, P., Rychliński, T., 2018. Solution-collapse breccias in the upper Olenekian–Ladinian succession, Tatra Mts, Poland. Annales Societatis Geologorum Poloniae, **88**: 303–319.

Jaglarz, P., Uchman, A., 2010. A hypersaline ichnoassemblage from the Middle Triassic carbonate ramp of the Tatricum domain in the Tatra Mountains, Southern Poland. Palaeogeography, Palaeoclimatology, Palaeoecology, **292**: 71–81.

Jeppsson, L., Anehus, R., 1995. A buffered formic acid technique for conodont extraction. Journal of Paleontology, **69**: 790–794.

Kaufmann, B., 2006. Calibrating the Devonian Time Scale: a synthesis of U–Pb ID–TIMS ages and conodont stratigraphy. Earth-Science Reviews, **76**: 175–190.

Lukševičs, E., Ahlberg, P. E., Stinkulis, Ģ., Vasiļkova, J., Zupiņš, I., 2011. Frasnian vertebrate taphonomy and sedimentology of macrofossil concentrations from the Langsēde Cliff, Latvia. Lethaia, **45**: 356–370.

Lukševičs, E., Stinkulis, Ģ., Mūrnieks, A., Popovs, K., 2012. Geological evolution of the Baltic Artesian Basin. In: Highlights of Groundwater Research in the Baltic Artesian Basin (eds. A. Dēliņa, et al.): 7–52. University of Latvia, Riga.

MacEachern, J.A., Bann, K.L., Gingras, M.K., Zonneveld, J.-P., Dashtgard, S.E., Pemberton, S.G., 2012. The ichnofacies paradigm. Developments in Sedimentology, **64**: 103–138. Elsevier, Amsterdam.

Mercedes-Martin, R., Buatois, L.A., 2021. Microbialites and trace fossils from a Middle Triassic restricted carbonate ramp in the Catalan Basin, Spain: evaluating environmental and evolutionary controls in an epicontinental setting. Lethaia, **54**: 4–25.

Matyja, H., 1993. Upper Devonian of Western Pomerania. Acta Geologica Polonica, **43**: 27–94.

Matyja, H., 2006. Stratigraphy and facies development of Devonian and Carboniferous deposits in the Pomeranian Basin and in the western part of the Baltic Basin and palaeogeography of the northern TESZ during late Paleozoic times (in Polish with English summary). Prace Państwowego Instytutu Geologicznego, **186**: 79–122.

Middleton, G.V., 1961. Evaporite solution breccias from the Mississippian of Southwest Montana. Journal of Sedimentary Petrology, **31**: 189–195.

Morrow, D.W., 1982. Descriptive field classification of sedimentary and diagenetic breccia fabrics in carbonate rocks. Bulletin of Canadian Petroleum Geology, **30**: 227–229.

Narbutas, V., 2005. Sedimentological–palaeogeographical maps for Stipinai age of the Middle Devonian. In: Evolution of Geological Environment in Lithuania (ed. A. Zuzevičius): 308. Institute of Geology and Geography, Vilnius University, Vilnius.

Ogg, J.G., Ogg, G.M., Gradstein, F.M., 2016. A Concise Geologic Time Scale: 2016. Elsevier, Amsterdam.

Paškevičius, J., 1997. The Geology of the Baltic Republics. Geological Survey of Lithuania, Vilnius.

Pemberton, S.G., Spila, M., Pulham, A. J., Saunders, T., MacEachern, J.A., Robbins, D., Sinclair, I.K., 2001. Ichnology and sedimentology of shallow to marginal marine systems: Ben Nevis and Avalon Reservoirs, Jeanne d'Arc Basin. Geological Association of Canada, Short Course Notes, **15**: 1–343.

Pontén, A., Plink-Björklund, P., 2009. Regressive to transgressive transits reflected in tidal bars, Middle Devonian Baltic Basin. Sedimentary Geology, **218**: 48–60.

Poprawa, P., Šliaupa, S., Stephenson, R., Lazauskienė, J., 1999. Late Vendian–Early Palaeozoic tectonic evolution of the Baltic Basin: regional tectonic implications from subsidence analysis. Tectonophysics, **314**: 219–239.

Raskatova, M., Jurina, A., 2012. Frasnian miospore assemblages and zones of Southern Latvia and North-Western Russia (Pskov Region). Scientific Papers University of Latvia – Earth and Environmental Sciences, **783**: 24–36.

Richardson, J.B., McGregor, D.C., 1986. Silurian and Devonian spore zones of the Old Red Sandstone Continent and adjacent regions. Geological Survey of Canada Bulletin, **364**: 1–79.

Rychliński, T., Jaglarz, P., Uchman, A., Vainorius, J., 2014. Unusually well preserved casts of halite crystals: a case from the Upper Frasnian of northern Lithuania. Sedimentary Geology, **308**: 44–52.

Sibley, D.F., Gregg, J.M., 1987. Classification of dolomite rock textures. Journal of Sedimentary Petrology, **57**: 967–975.

Sorokin, V.S., 1978. Etapy razvitiya Severo-zapada Russkoy platformy vo franskom veke (in Russian). Zinatne, Riga.

Stinkulis, Ģ., Lukševičs, E., Reķe, T., 2020. Sedimentology and vertebrate fossils of the Frasnian Ogre Formation, Gurova outcrops, eastern Latvia. Estonian Journal of Earth Sciences, **69**: 248–261.

Streel, M., Higgs, K., Loboziak, S., Riegel, W., Steemans, P., 1987. Spore stratigraphy and correlation with faunas and floras in the type marine Devonian of the Ardenne-Rhenish regions. Review Palaeobotany and Palynology, **50**: 211–229.

Streel, M., Boulvain, F., Dusar, M., Loboziak, S., Steemans, P., 2021. Updating Frasnian miospore zonation from the Boulonnais (Northern France) and comparison with new data from the Upper Palaeozoic cover on the Brabant Massif (Western Belgium). Geologica Belgica, **24**: 69-84.

Strother, P.K., 1996. Acritarchs. In: Palynology: Principles and Applications 1 (eds. J. Jansonius and D.C. McGregor): 81–106. American Association of Stratigraphic Palynologists Foundation, Publishers Press, Salt Lake City, Utah.

Sweet, W.C., 1988. The Conodonta: Morphology, Taxonomy, Palaeoecology, and Evolutionary History of a Long-Extinct Animal Phylum. Oxford Monographs on Geology and Geophysics, **10**, Clarendon Press, Oxford.

Swennen, R., Viaene, W., Cornelissen, C., 1990. Petrography and geochemistry of the Belle Roche breccia (lower Visean, Belgium): evidence for brecciation by evaporite dissolution. Sedimentology, **37**: 859–878.

Tänavsuu-Milkeviciene, K., Plink-Björklund, P., Kirsimäe, K., 2008. Synsedimentary brecciation in the Eifelian (Middle Devonian) Baltic Basin: sudden catastrophe or diagenetic collapse? Terra Nova, **20**: 449–454.

Tänavsuu-Milkeviciene, K., Plink-Björklund, P., Kirsimäe, K., Ainsaar, L., 2009. Coeval versus reciprocal mixed carbonate–siliciclastic deposition, Middle Devonian Baltic Basin, Eastern Europe: implications from the regional tectonic development. Sedimentology, **56**: 1250–1274.

Ūsaitytė, D., 2000. The geology of the southeastern Baltic Sea: a review. Earth-Science Reviews, **50**: 137–225.

Vodzinskas, E., Kadūnas, V., 1969. Carbonaceous raw material of the Lithuanian SSR (dolomites and limestones) (in Russian with English summary). Publishing Office "Minitis", Vilnius.

Wood, G.D., Turnau, E., 2001. New Devonian Cenobial Chlorococcales (Hydrodictyaceae) from the Holy Cross mountains and Radom-Lublin region of Poland: Their paleoenvironmental and sequence stratigraphic implications. In: Proceedings of the IX International Palynological Congress, Houston, Texas, U.S.A., 1996 (eds. D.K. Goodman and R.T. Clark): 53–63. American Association of Stratigraphic Palynologists Foundation, Dallas, Texas.

Wood, G.D., Gabriel, A.M., Lawson, J.C., 1996. Palynological techniques – processing and microscopy. In: Palynology: Principles and Applications (eds. J. Jansonius and D.C. McGregor), **1**: 29–50. American Association of Stratigraphic Palynologists Foundation, Dallas, Texas.

Wright, V.P., 1990. A micromorphological classification of fossil and recent calcic and petrocalcic microstructures. In: Soil Micromorphology: a Basic and Applied Science (ed. L.A. Douglas): 401–407. Developments in Soil Science, Elsevier, Amsterdam.

Zatoń, M., Borszcz, T., Berkowski, B., Rakociński, M., Zapalski, M.K., Zhuravlev, A.V., 2015. Paleoecology and sedimentary environment of the Late Devonian coral biostrome from the Central Devonian Field, Russia. Palaeogeography, Palaeoclimatology, Palaeoecology, **424**:61–75.

Ziegler, P.A., 1988. Evolution of the Arctic–North-Atlantic and the Western Tethys. AAPG Memoir, **43**: 198.

Ziegler, W., Sandberg, C.A., 1990. The late Devonian standard conodont zonation. Courier Forschungsinstitut Senckenberg, **121**: 1–115.